Supplementary Information for

A direct reaction approach for the synthesis of zeolitic imidazolate frameworks: template and temperature mediated control on network topology and crystal size

*Mónica Lanchas,[a] Daniel Vallejo-Sánchez,[a] Garikoitz Beobide,[*a] Oscar Castillo,[*a] Andrés T. Aguayo,[b] Antonio Luque[a] and Pascual Román[a]*

[a]Departamento de Química Inorgánica, Facultad de Ciencia y Tecnología, Universidad del País Vasco, UPV/EHU, Apartado 644, E–48080 Bilbao, Spain and [b] Departamento de Ingeniería Química, Facultad de Ciencia y Tecnología, UPV/EHU, Universidad del País Vasco, Apartado 644, E–48080 Bilbao, Spain.

S1. SOLVENT FREE SYNTHESIS OF M(II)-IMIDAZOLATES (M: Zn, Co)

Chemicals

All the chemicals were of reagent grade and were used as commercially obtained.

Synthesis

Samples were prepared according to the following general procedure. The corresponding amounts of the metal source (ZnO, $Co(OH)_2$, or CoO) and the bridging ligand (imidazole or 2-methylimidazole) were hand-grinded thoroughly to obtain a homogeneous mixture. When necessary, the structure directing agent (1-butanol, pyridine, 4-methylpyridine) was added to the mixture prior to be grinded. The final mixture was sealed in a 45-mL Teflon-lined autoclave and heated with the thermal programs described in Table S1.1. Table S1.2 shows the details on the preparation of each sample. The products were washed with ethanol to remove unreacted imidazole and 2-methylimidazole (or remains of the template molecule) and sequentially characterized by elemental analysis, FTIR spectroscopy, thermogravimetric analysis (TGA) and X-ray powder diffraction (XRPD).

The discrepancies among the calculated and experimental values of the elemental analyses (Table S2.1) are attributed to the presence of unreacted metal oxide or hydroxide that range between 3 and 13% (wt%). The reaction yields were calculated from the thermogravimetric data, on the basis of the weight of the final residue and the weight of the metal imidazolate once it has lost all guest molecules. The identification of the metal imidazolate crystal structure was made scrutinizing the Cambridge Structural Database on the basis of the experimental XRPD data of the synthesized samples (for further details see section S4).

Effect of the heating rate in the features of the synthesized product and in the growth of x-ray quality single crystals is discussed in section S5, while details concerning single crystal x-ray diffraction data collection and structure determination of the compound $\{[Co(Im)_2]\cdot(H_2O)_{2.5}\cdot(4mPy)_{0.2}\}_n$ are gathered in section S6.

Physical Measurements

The purity and homogeneity of the polycrystalline samples were checked by elemental analysis, IR spectroscopy, thermogravimetric measurements and X-ray powder diffraction methods. Elemental analyses (C, H, N) were performed on a Euro EA Elemental Analyzer, whereas the metal content determined by a Horiba Yobin Yvon Activa inductively coupled plasma atomic emission spectrometer (ICP-AES). The IR spectra (KBr pellets) were recorded on a FTIR 8400S Shimadzu spectrometer in the 4000–400 cm^{-1} spectral region. Thermal analyses (TG/DTA) were performed on a TA Instruments SDT 2960 thermal analyzer in a synthetic air atmosphere (79% N_2 / 21% O_2) with a heating rate of 5ºC min^{-1}.

Table S1.1. Employed thermal programs.

Thermal program number	Thermal Steps
1	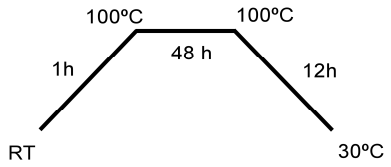
2	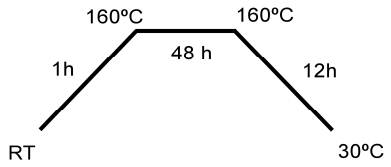
3	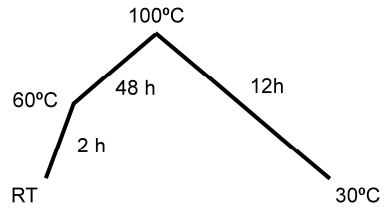
4	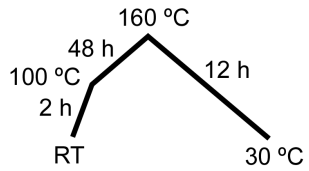

Table S1.2. Synthesis conditions, formulae of the synthesised imidazolate, yield and corresponding CSD (Cambridge Structural Database) code.[1]

M:Im:T	Synthesis ratio	Reactants	Thermal program	T (ºC)	Formulae	Yield (%)	CSD
Zn:Im	1:2.1	*ZnO*: 4 mmol *Im*: 8.4 mmol	1	100	$[Zn_4(Im)_8(Him)]_n$	92.3	KUMXEW
Zn:Im	1:2.1	*ZnO*: 4 mmol *Im*: 8.4 mmol	2	160	$[Zn(Im)_2]_n$	87.2	IMDZB02
Zn:Im:But	1:2.1:2.5	*ZnO*: 8 mmol *Im*: 16.8 mmol *But*: 20 mmol	1	100	$[Zn(Im)_2]_n$	97.4	IMDZB07
Co:Im:Py	1:2.1:2.5	*Co(OH)$_2$*: 8 mmol *Im*: 16.8 mmol *Py*: 20 mmol	1/3	100	$\{[Co(Im)_2]\cdot(Py)_{0.5}\}_n$	96.9	EQOBUH
Zn:Im:Py	1:2.1:2.5	*ZnO*: 8 mmol *Im*: 16.8 mmol *Py*: 20 mmol	1/3	100	$\{[Zn(Im)_2]\cdot(Py)_{0.5}\}_n$	94.5	*This work*
Zn:Im:4mPy	1:2.1:2.5	*ZnO*: 8 mmol *Im*: 16.8 mmol *4mPy*: 20 mmol	3	100	$[Zn(Im)_2]_n$	91.3	KUMXEW
Co:Im:4mPy	1:2.1:2.5	*Co(OH)$_2$*: 8 mmol *Im*: 16.8 mmol *4mPy*: 20 mmol	3	100	$\{[Co(Im)_2]\cdot(H_2O)_{2.5}\cdot(4mPy)_{0.2}\}_n$	96.5	*This work*
Zn:mIm	1:2.1	*ZnO*: 4 mmol *mIm*: 8.4 mmol	4	160	$\{[Zn(mIm)_2]\cdot(H_2O)_{0.5}\}_n$	93.8	TUDHUW
Co:mIm	1:2.1	*Co(OH)$_2$*: 4 mmol *mIm*: 8.4 mmol	4	160	$\{[Co(mIm)_2]\cdot(H_2O)_{0.8}\}_n$	87.3	GITTOT01
Co:mIm	1:2.1	*CoO*: 4 mmol *mIm*: 8.4 mmol	4	160	$\{[Co(mIm)_2]\cdot H_2O\}_n$	67.2	GITTOT01

[1]: *Im*: imidazole; *mIm*: 2-methylimidazole; *But*: 1-butanol; *4mPy*: 4-methylpyridine; *Py*: pyridine;

S2. ELEMENTAL ANALYSES AND FTIR SPECTRA

Table S2.1. Results of the elemental analyses and main FTIR bands for each sample. *

M:Im:T	Syn. ratio	T (ºC)	Formulae	Elemental Analysis (%)	***Main FTIR bands*** (cm^{-1}, KBr pellets)
Zn:Im	1:2.1	100	$[Zn_4(Im)_8(Him)]_n$ $[Zn_4(C_3H_3N_2)_8(C_3H_4N_2)]_n$	Calcd: C, 37.44; H, 3.26; N, 29.10; Zn: 30.20. Found: C, 36.83; H, 3.07; N, 28.77; Zn: 30.82	3450 (m), 3129 (w), 3114 (w), 1615 (w), 1497 (s), 1476 (s), 1400 (w), 1383 (m), 1321 (w), 1280 (w), 1241 (m), 1173 (m), 1103 (s), 1094 (vs), 1088 (vs), 1076 (s) 977 (w), 954 (s), 840 (w), 831 (m), 768 (m), 755 (s), 670 (s), 620 (w), 490 (vw).
Zn:Im	1:2.1	160	$[Zn(Im)_2]_n$ $[Zn(C_3H_3N_2)_2]_n$	Calcd: C, 36.12; H, 3.03; N, 28.08; Zn: 32.77 Found: C, 34.60; H, 2.77; N, 26.97; Zn: 34.02	3442 (w), 3144 (w), 3132 (w), 3109 (w), 1667 (w), 1610 (w), 1493 (s), 1472 (s), 1400 (w), 1384 (w), 1321 (m), 1283 (w), 1240 (m), 1170 (m), 1089 (vs), 980 (w), 953 (s), 858 (w), 833 (m), 775 (m), 756 (s), 669 (s), 647 (w), 470 (w).
Zn:Im:But	1:2.1:2.5	100	$[Zn(Im)_2]_n$ $[Zn(C_3H_3N_2)_2]_n$	Calcd: C, 36.12; H, 3.03; N, 28.08; Zn: 32.77 Found: C, 35.03; H, 2.81; N, 27.68; Zn: 34.83	3425 (w), 3133 (w), 3111 (w), 2972 (w), 2928 (w), 1660 (w), 1610 (w), 1495 (s), 1470 (s), 1402 (w), 1384 (w), 1319 (m), 1282 (w), 1242 (w), 1171 (m), 1091 (vs), 977 (w), 952 (s), 832 (m), 761 (s), 668 (s), 647 (w), 560 (w).
Zn:Im:Py	1:2.1:2.5	100	$\{[Zn(Im)_2]\cdot(Py)_{0.5}\}_n$ $\{[Zn(C_3H_3N_2)_2]\cdot(C_5H_5N)_{0.5}\}_n$	Calcd: C, 42.70; H, 3.58; N, 26.36; Zn: 27.35 Found: C, 41.33; H, 3.47; N, 25.51; Zn: 29.07	3440 (m), 3130 (w), 3108 (w), 1667 (w), 1600 (w), 1497 (s), 1472 (s), 1437 (w), 1400 (w), 1384 (m),), 1321 (w), 1283 (w), 1238 (m), 1170 (m), 1090 (vs), 975 (w), 953 (s), 833 (m), 756 (s), 705 (w), 669 (s), 528 (w), 470 (vw)
Co:Im:Py	1:2.1:2.5	100	$\{[Co(Im)_2]\cdot(Py)_{0.5}\}_n$ $\{[Co(C_3H_3N_2)_2]\cdot(C_5H_5N)_{0.5}\}_n$	Calcd: C, 43.89; H, 3.68; N, 27.10; Co: 25.33 Found: C, 42.98; H, 3.57; N, 26.52; Co: 26.83	3440 (m), 3147 (w), 3130 (w), 3108 (w), 1667 (w), 1600 (w), 1578 (m), 1570 (w), 1497 (s), 1472 (s), 1435 (m), 1400 (w), 1384 (m),1211 (w), 1090 (vs), 1028 (w), 989 (w), 975 (w), 953 (s), 833 (m), 860 (w), 775 (m), 756 (s), 706 (m), 669 (s), 647 (w), 600 (w), 470 (vw), 428 (w).

* The analysis has been performed over the the washed final mixture that is composed mainly of the ZIF product (87-97%) but also of the unreacted metal source (ZnO, CoO and $Co(OH)_2$).

Table S2.2. Results of the elemental analyses and main FTIR bands for each sample.*

M:Im:T	Syn. ratio	T (ºC)	Formulae	Elemental Analysis (%)	***Main FTIR bands*** (cm^{-1}, KBr pellets)
Zn:Im:4mPy	1:2.1:2.5	100	$[Zn(Im)_2]_n$ $[Zn(C_3H_3N_2)_2]_n$	Calcd: C, 36.12; H, 3.03; N, 28.08; Zn: 32.77 Found: C, 39.88; H, 4.40; N, 23.41; Zn: 28.01	3453 (s), 3110 (sh), 1980 (w), 1631 (m), 1497 (s), 1477 (s), 1400 (m), 1385 (m), 1320 (w), 1280 (w), 1244 (m), 1170 (m), 1105 (s), 1094 (vs), 1088 (vs), 1076 (s), 978 (w), 954 (s), 840 (m), 831 (m), 767 (s), 756 (s), 669 (s), 489 (m).
Co:Im:4mPy	1:2.1:2.5	100	$\{[Co(Im)_2]\cdot(H_2O)_{1.6}\cdot(4mPy)_{0.2}\}_n$ $\{[Co(C_3H_3N_2)_2]\cdot(H_2O)_{1.6}(C_6H_7N)_{0.2}\}_n$	Calcd: C, 35.95; H, 4.44; N, 24.46; Co: 24.50 Found: C, 35.06; H, 4,30; N, 23.82; Co: 26.06	3440 (m), 3147 (w), 3130 (w), 3108 (w), 1667 (w), 1600 (w), 1578 (m), 1570 (w), 1497 (s), 1472 (s), 1435 (m), 1400 (w), 1384 (m),1211 (w), 1090 (vs), 1028 (w), 989 (w), 975 (w), 953 (s), 833 (m), 860 (w), 775 (m), 756 (s), 706 (m), 669 (s), 647 (w), 600 (w), 470 (vw), 428 (w).
Zn:mIm	1:2.1	160	$\{[Zn(mIm)_2]\cdot(H_2O)_{0.5}\}_n$ $\{[Zn(C_4H_5N_2)_2]\cdot(H_2O)_{0.5}\}_n$	Calcd: C, 40.61; H, 4.69; N, 23.68; Co: 27.64 Found: C, 39.98; H, 3.97; N, 22.82; Co: 29.37	3421 (m), 3130 (m), 2964 (w), 2930 (w), 1648 (sh), 1590 (m), 1509 (w), 1458 (s), 1422 (vs), 1383 (m), 1308 (s), 1180 (m), 1147 (s), 1092 (w), 994 (m), 953 (w), 838 (w), 758 (m), 694 (m), 684 (m), 669 (w), 421 (s).
Co:mIm	1:2.1	160	$\{[Co(mIm)_2]\cdot(H_2O)_{0.8}\}_n$ $\{[Co(C_4H_5N_2)_2]\cdot(H_2O)_{0.5}\}_n$	Calcd: C, 40.79; H, 4.96; N, 23.79; Co: 25.02 Found: C, 38.91; H, 4.83; N, 22.68; Co: 28.11	3421 (m), 3130 (m), 2962 (w), 2924 (w), 1633 (sh), 1578 (m), 1507 (w), 1454 (s), 1414 (vs), 1383 (m), 1303 (s), 1172 (m), 1139 (s), 1087 (w), 992 (m), 950 (w), 835 (w), 750 (m), 692 (m), 683 (sh), 669 (w), 659 (w), 561 (w) 507 (sh), 425 (s).
Co:mIm	1:2.1	160	$\{[Co(mIm)_2]\cdot H_2O\}_n$ $\{[Co(C_4H_5N_2)_2]\cdot H_2O\}_n$	Calcd: C, 40.18; H, 5.06; N, 23.43; Co: 24.64 Found: C, 34.16; H, 4,62; N, 18.82; Co: 32.09	3421 (m), 3130 (m), 2962 (w), 2924 (w), 1633 (sh), 1578 (m), 1507 (w), 1454 (s), 1414 (vs), 1383 (m), 1303 (s), 1172 (m), 1139 (s), 1087 (w), 992 (m), 950 (w), 835 (w), 750 (m), 692 (m), 683 (sh), 561 (w) 507 (sh), 425 (s).

* The analysis has been performed over the the washed final mixture that is composed mainly of the ZIF product (87-97%) but also of the unreacted metal source (ZnO, CoO and $Co(OH)_2$).

S3. THERMOGRAVIMETRY AND DIFERENTIAL THERMAL ANALYSIS

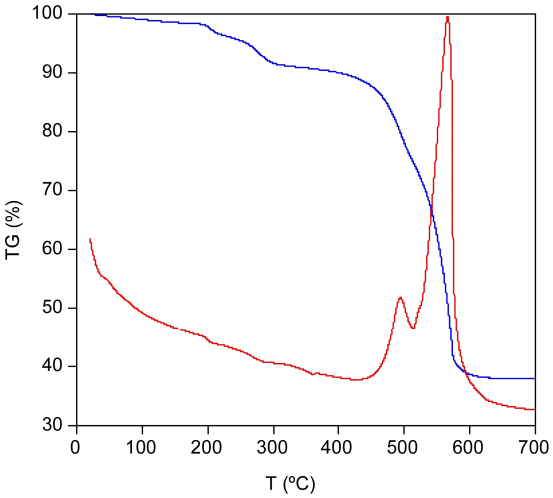

Zn:Im 1:2.1 (100 ºC)

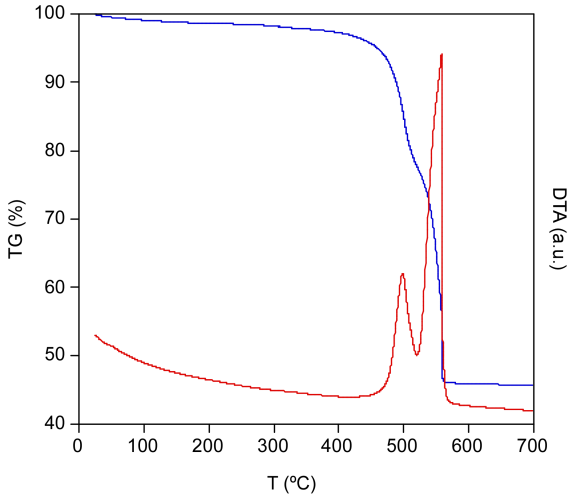

Zn:Im 1:2.1 (160 ºC)

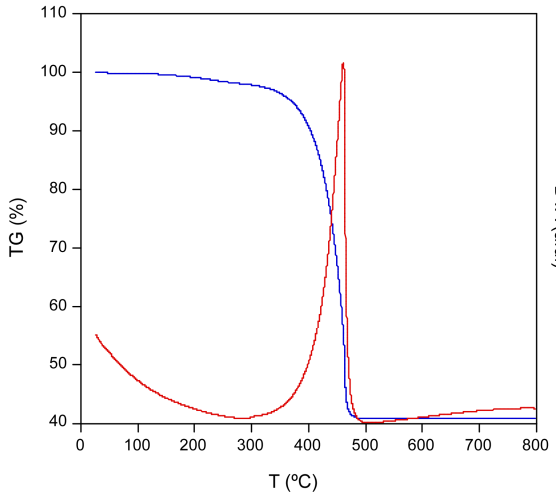

Zn:Im:But 1:2.1:2.5 (100 ºC)

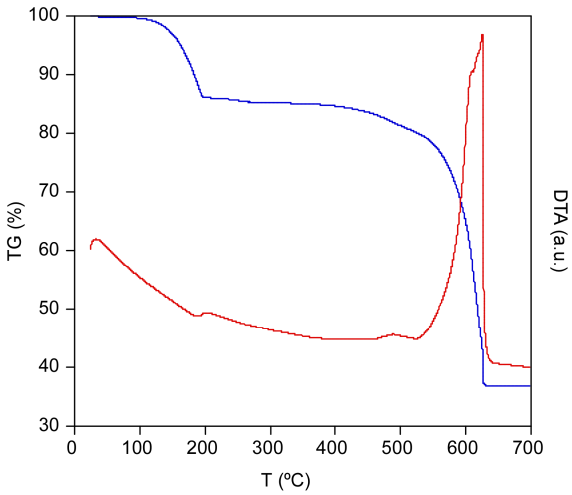

Zn:Im:Py 1:2.1:2.5 (100 ºC)

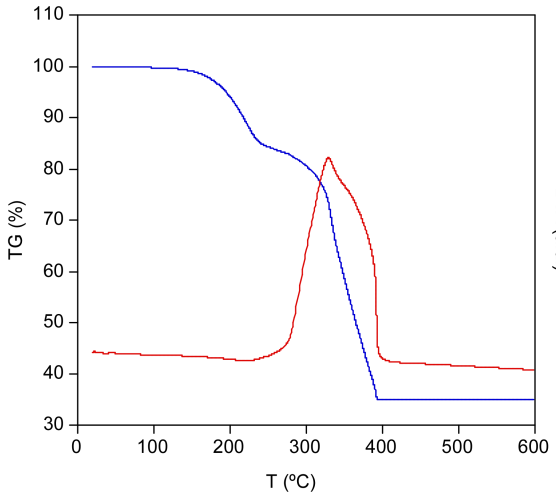

Co:Im:Py 1:2.1:2.5 (100 ºC)

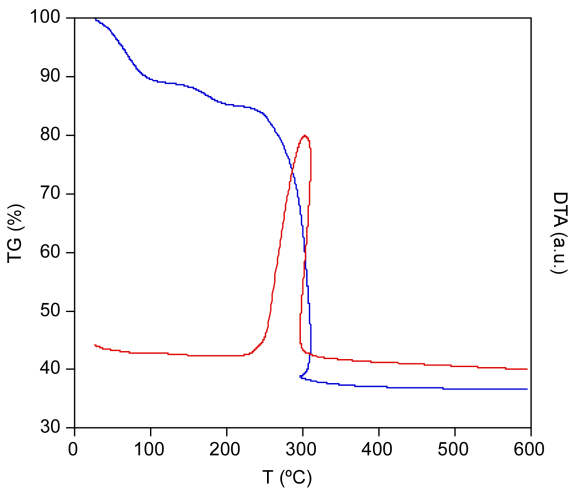

Co:Im:mPy 1:2.1:2.5 (100 ºC)

Figure S3.1. Thermogravimetric measurements performed upon Zn(II) and Co(II) imidazolates.

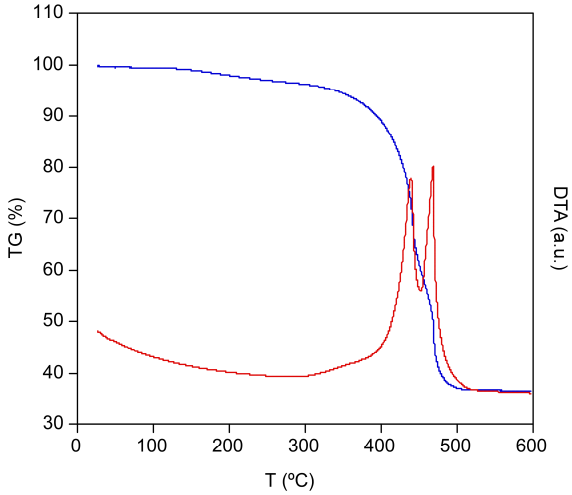

Zn:mIm 1:2.1 (160 ºC)

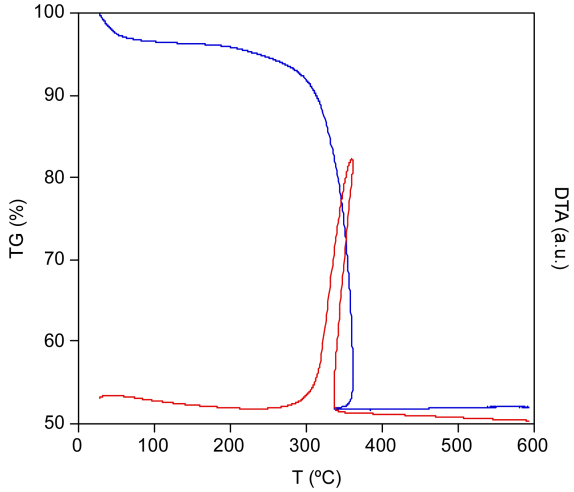

Co:mIm 1:2.1 (160 ºC)

Co source: CoO

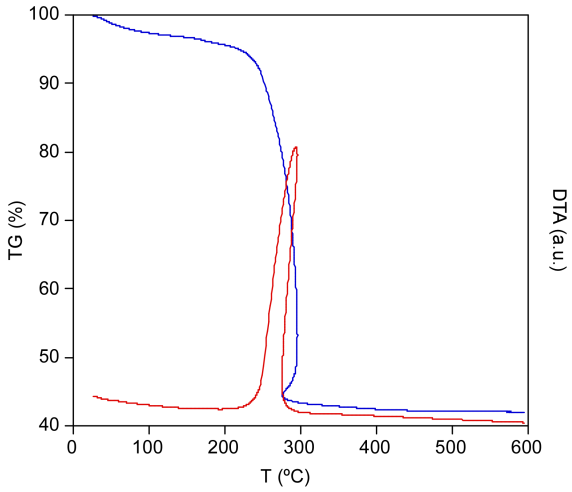

Co:mIm 1:2.1 (160 ºC)

Co source: $Co(OH)_2$

Figure S3.2. Thermogravimetric measurements performed upon Zn(II) and Co(II) 2-methylimidazolates.

S4. X-RAY POWDER DIFRACTION ANALYSIS

The X-ray powder diffraction (XRPD) patterns were collected on a Phillips X'PERT powder diffractometer with Cu-Kα radiation (λ = 1.5418 Å) over the range 5 < 2θ < 70 with a step size of 0.02º and an acquisition time of 2.5 s per step at 20 ºC. Indexation of the diffraction profiles was made by means of the FULLPROF program (pattern-matching analysis)[1] on the basis of the space group and the cell parameters found in the *Cambridge Structural Database* (*CSD*) for the metal-imidazolates (elucidated by single crystal X-ray diffraction) and found in the *Inorganic Crystal Structure Database* (*ICSD*) for the corresponding metal oxide or hydroxide precursor. The calculated and observed diffraction patterns are shown in Figures S4.1-S4.7.

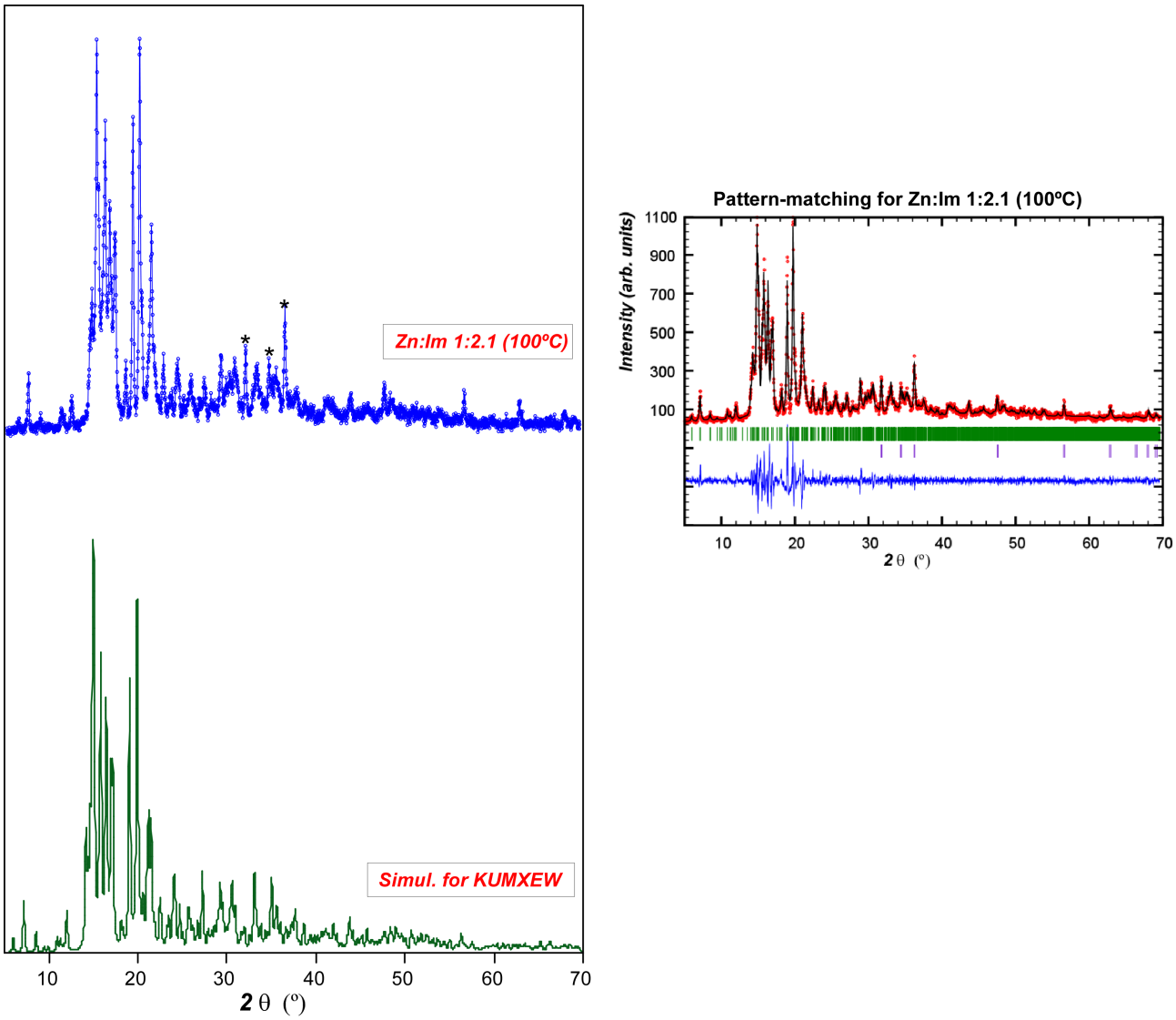

Figure S4.1. *Left*: comparison between the simulated XRPD of *KUMXEW* and the experimental XRPD of Zn:Im sample prepared at 100 ºC. "*" indicates the most intense peaks of ZnO. *Right*: pattern-matching refinement (green ticks: calculated reflections of zinc imidazolate phase; purple ticks: calculated reflections of ZnO).

[1] **(a)** Rodríguez-Carvajal, J. *FULLPROF*, *Program Rietveld for Pattern Matching Analysis of Powder Patterns*, Abstacts of the Satellite Meeting on Powder Diffraction of the XV Congress of the IUCr, Toulouse, Francia, **1990**, 127. **(b)** Rodríguez-Carvajal, J.: *FULLPROF 2000*, version 2.5d, Laboratoire Léon Brillouin (CEA-CNRS), Centre d'Études de Saclay, Gif sur Yvette Cedex, Francia, **2003**.

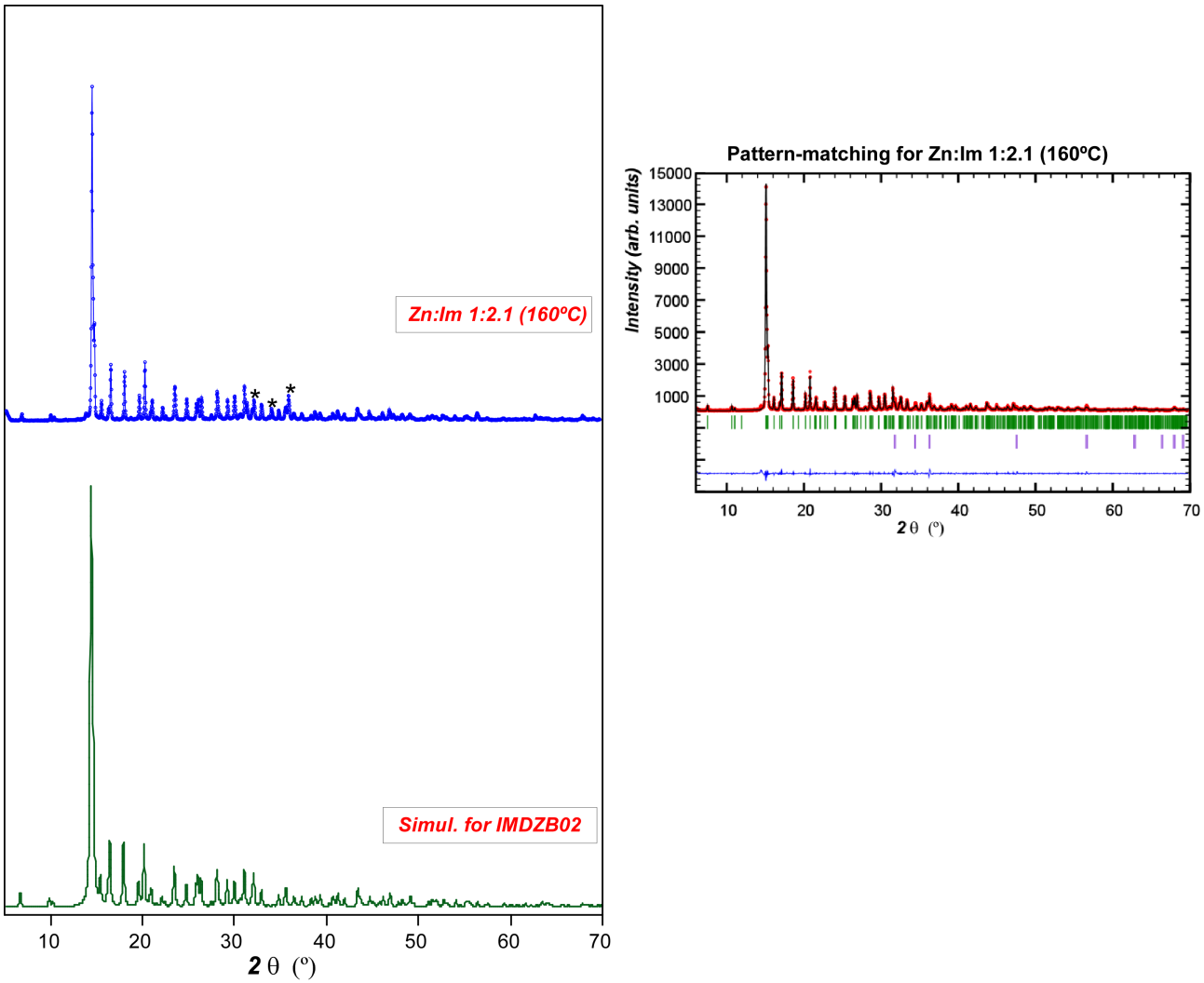

Figure S4.2. *Left*: comparison between the simulated XRPD of *IMDZB02* and the experimental XRPD of Zn:Im sample prepared at 160 ºC. "*" indicates the most intense peaks of ZnO. *Right*: pattern-matching refinement of the experimental data (green ticks: calculated reflections of zinc imidazolate phase; purple ticks: calculated reflections of ZnO).

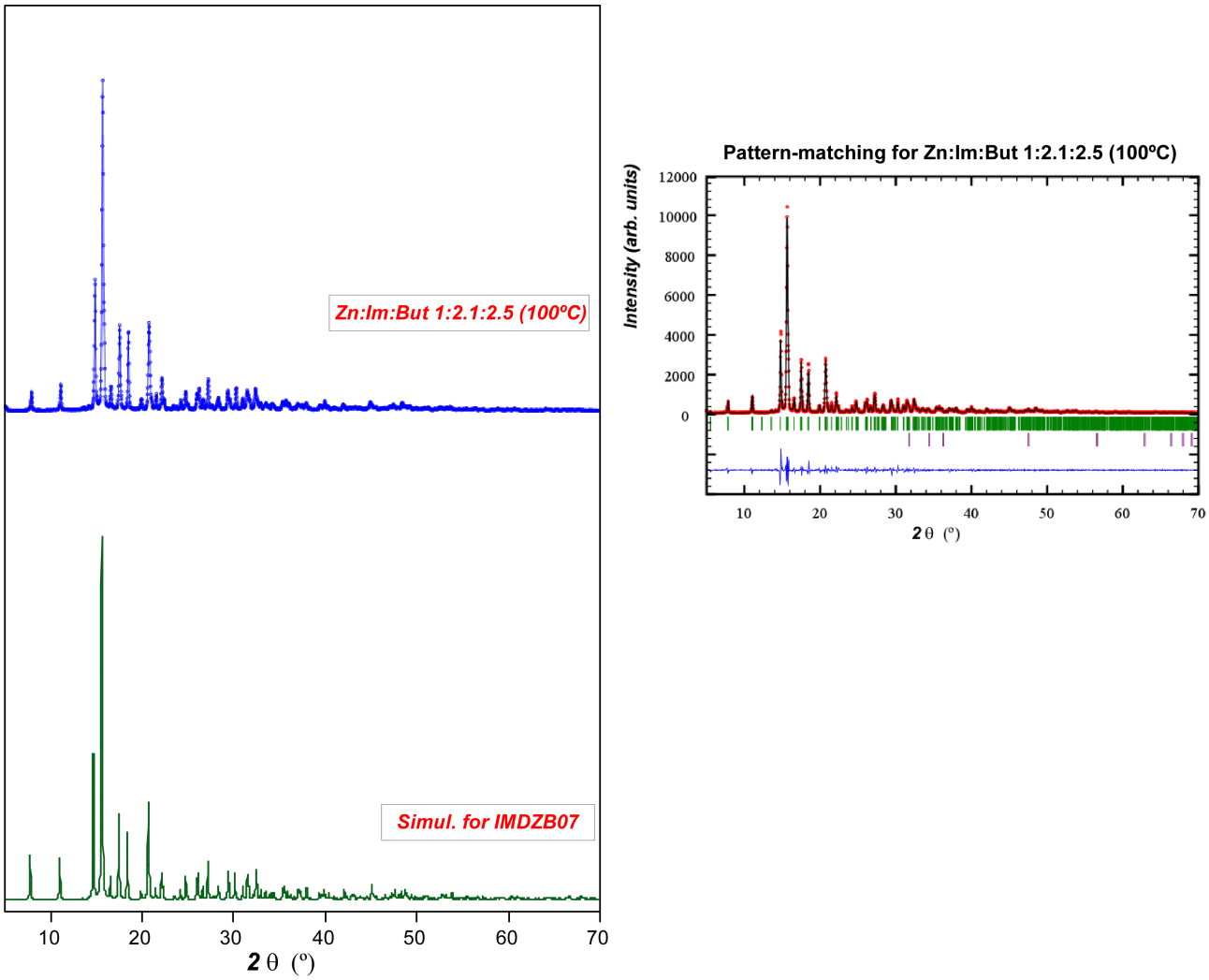

Figure S4.3. *Left*: comparison between the simulated XRPD of *IMDZB07* and the experimental XRPD of Zn:Im:But sample prepared at 100 ºC. Non peaks of ZnO where detected on the XRPD pattern. *Right*: pattern-matching refinement of the experimental data (green ticks: calculated reflections of zinc imidazolate phase; purple ticks: calculated reflections of ZnO).

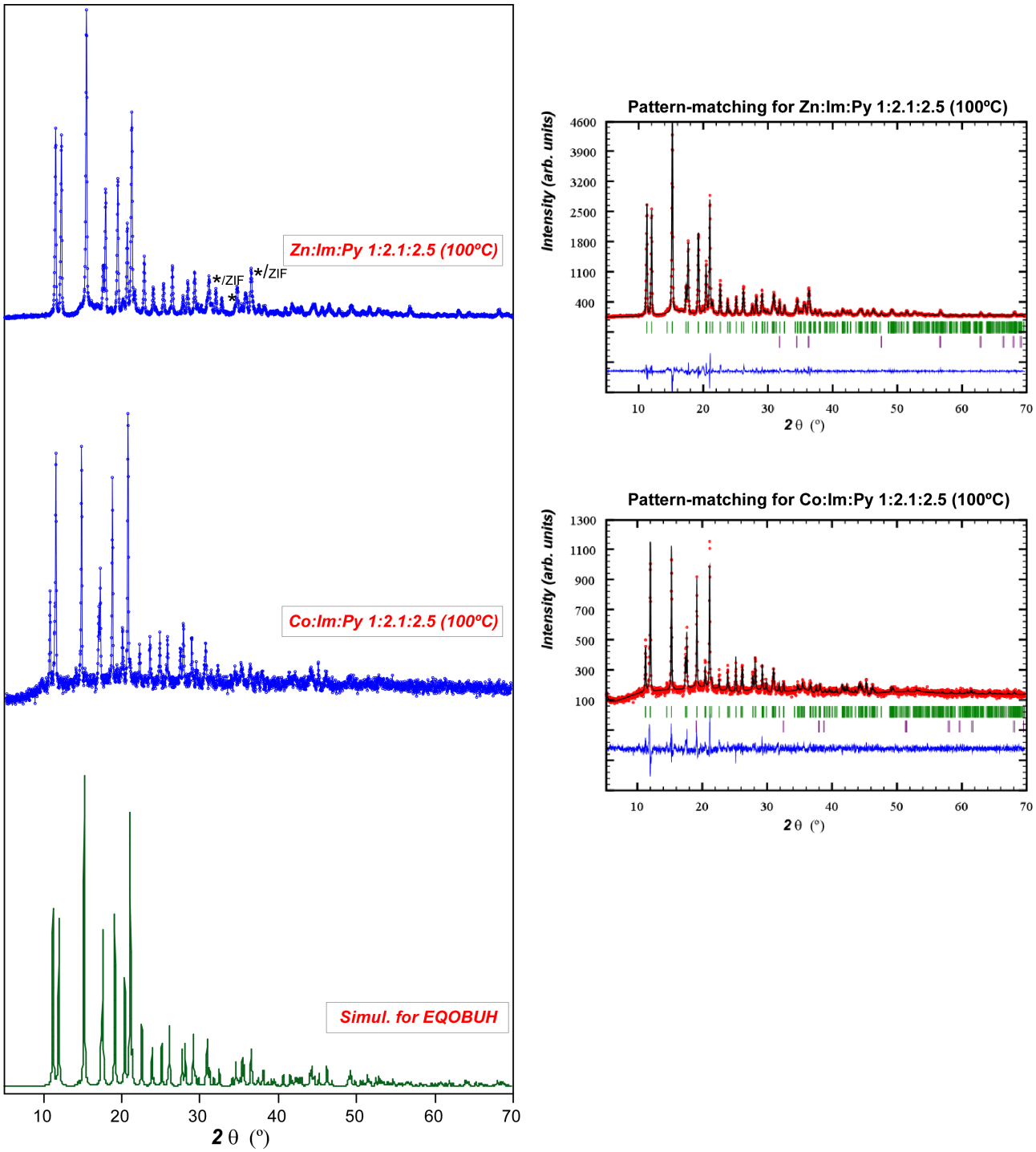

Figure S4.4. *Left*: comparison between the simulated XRPD of *EQOBUH* and the experimental XRPD of M:Im:Py (M(II): Co, Zn) samples prepared at 100 ºC. "*" indicates the most intense peaks of ZnO. Non peaks of $Co(OH)_2$ where detected on the XRPD pattern. *Right*: pattern-matching refinement of the experimental data (green ticks: calculated reflections of cobalt imidazolate phase; purple ticks: calculated reflections of ZnO (upper figure) or $Co(OH)_2$ (lower figure)).

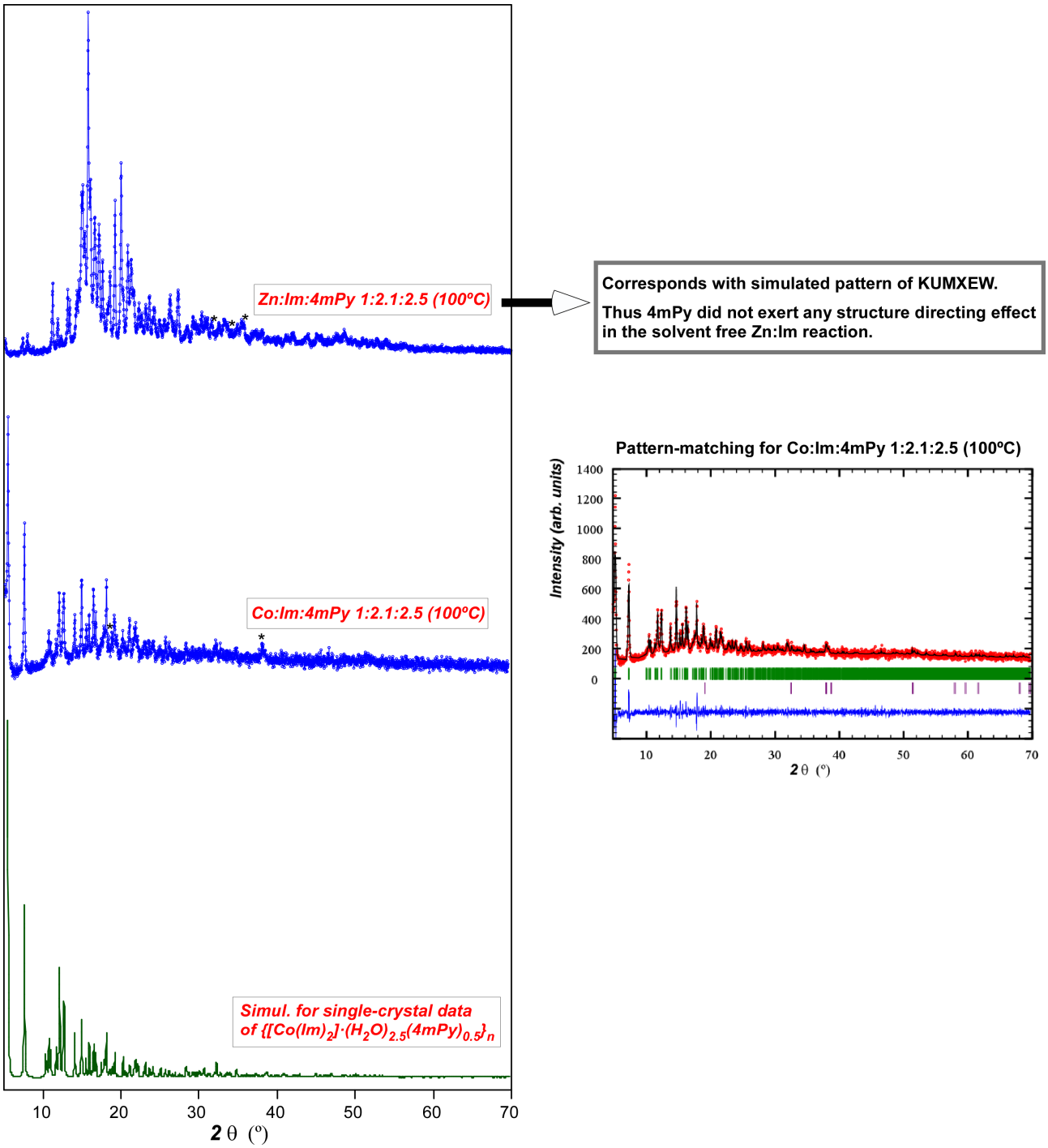

Figure S4.5. *Left*: comparison between the simulated XRPD of $\{[Co(Im)_2]\cdot(H_2O)_{2.5}\cdot(4mPy)_{0.2}\}_n$ and the experimental XRPD of M:Im:4mpy (M(II): Co, Zn) samples prepared at 100 ºC. "*" indicates the most intense peaks of $Co(OH)_2$ or ZnO. *Right*: pattern-matching refinement of the experimental data (green ticks: calculated reflections of cobalt imidazolate phase; purple ticks: calculated reflections of $Co(OH)_2$).

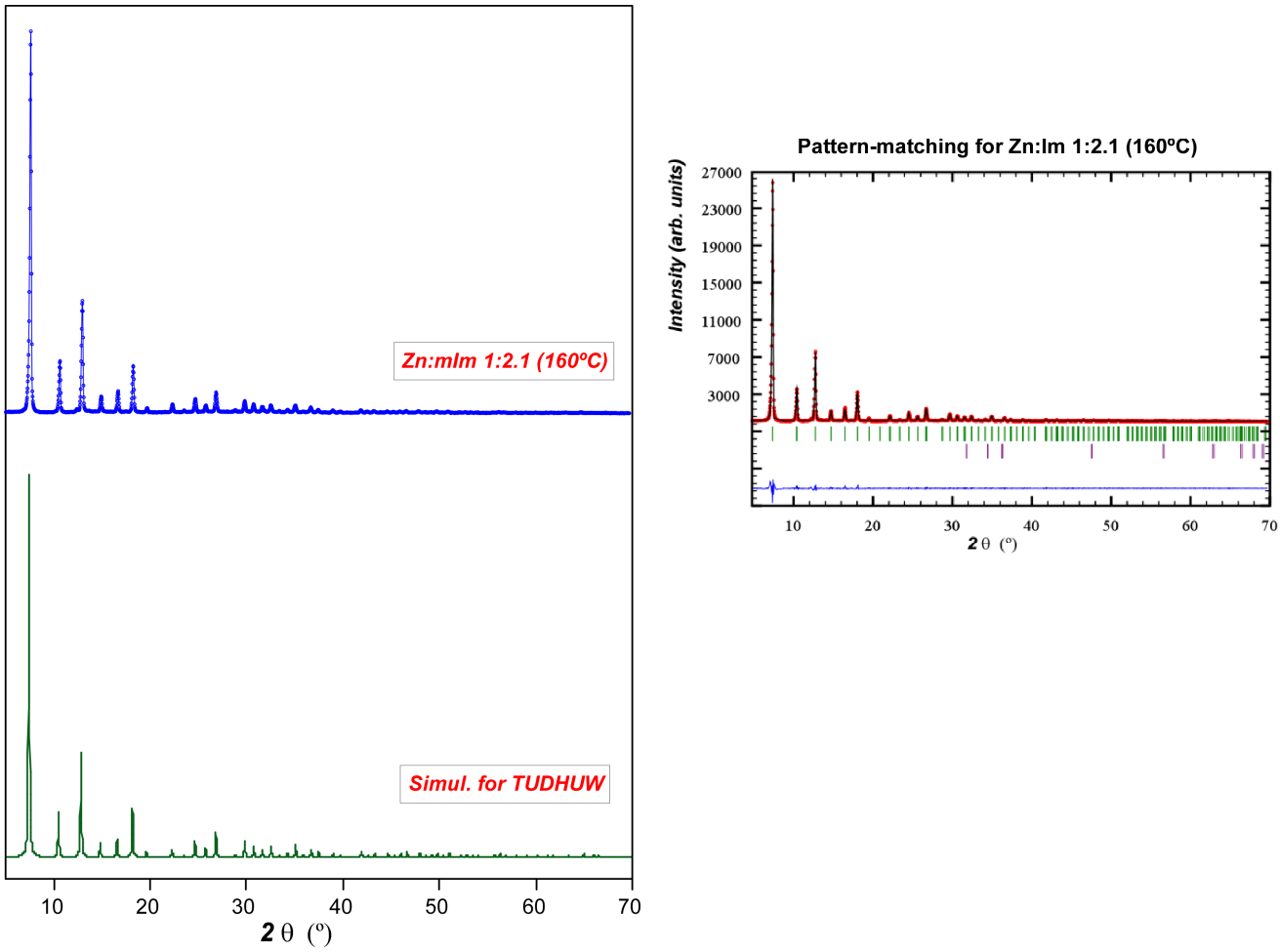

Figure S4.6. *Left*: comparison between the simulated XRPD of TUDHUW and the experimental XRPD of Zn:mIm sample prepared at 160 ºC. Non peaks of $Co(OH)_2$ where detected on the XRPD pattern. *Right*: pattern-matching refinement of the experimental data (green ticks: calculated reflections of zinc imidazolate phase; purple ticks: calculated reflections of ZnO).

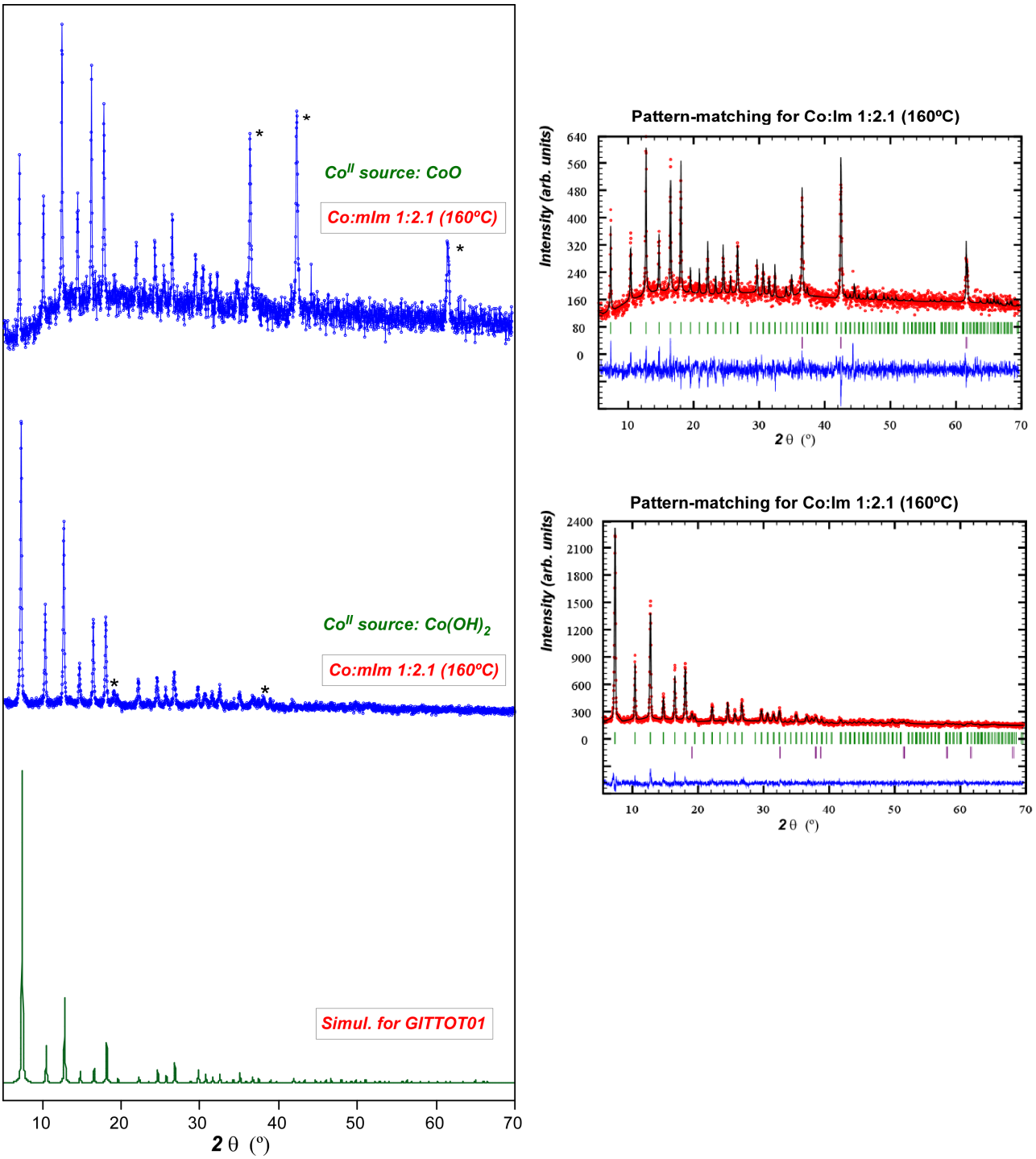

Figure S4.7. *Left*: comparison between the simulated XRPD of GITTOT01 and the experimental XRPD of Co:mIm samples prepared at 160 ºC from CoO and $Co(OH)_2$ precursors. The asterisks indicate peaks corresponding to unreacted CoO. *Right*: pattern-matching refinement of the experimental data (green ticks: calculated reflections of cobalt imidazolate phase; purple ticks: calculated reflections of CoO (upper figure) and $Co(OH)_2$ (lower figure)). "*" indicates the most intense peaks of CoO or $Co(OH)_2$.

S5. CRYSTALLOGRAPHIC DATA AND PROFILE REFINEMENT DATA FOR $\{[Zn(Im)_2]\ (Py)_{0.5}\}_n$

$\{[Zn(Im)_2]\cdot(Py)_{0.5}\}_n$ is isotructural to its analogous Co(II) compound for which the crystal structure was previously described[2] (CSD code: EQOBUH). As far as we know there is no report of compound $\{[Zn(Im)_2]\ (Py)_{0.5}\}_n$. Therefore, herein we report the results of the Lebail fitting of its XRPD data for the cell parameters (Table S5.1). A figure showing the fitting of the experimental XRPD data, the calculated one and the difference between them is shown in the previous section (Figure S4.4), while the results of the chemical and thermal analyses are collected in sections S2 and S3.

Table S5.1. Crystallographic data, data collection parameters and structure refinement details of compound $\{[Zn(Im)_2]\cdot(Py)_{0.5}\}_n$.

Empirical formula	$C_{8.5}H_{8.5}N_{4.5}Zn$	**Temperature (K)**	293(2)
Formula weight	239.08	$\lambda_{CuK\alpha}$ **(Å)**	1.5406
Crystal system	Orthorombic	**2θ Range (°)**	$10 < 2\theta < 70$
Space Group	*Fdd2*	**Δ2θ / step (°)**	0.03
***a* (Å)**	18.473(1)	R_f	1.54
***b* (Å)**	24.573(1)	R_{Bragg}	1.15
***c* (Å)**	9.295(1)	χ^2	2.32
V (Å^3)	4219.4(4)		

$$R_f = \frac{\sum\left|\sqrt{I_{obs}} - \sqrt{I_{calc}}\right|}{\sum\sqrt{I_{obs}}}\ ;\ R_{Bragg} = \frac{\sum\left|I_{obs} - I_{calc}\right|}{\sum I_{obs}}$$

[2] Y. -Q. Tian,C. -X. Cai, X.-M. Ren, C. -Y. Duan, Y. Xu, S. Gao, X. -Z. You, *Chem.-Eur.J.*, **2003**, *9*, 5673.

S6. EFFECT OF THE HEATING RATES ON SAMPLE CRYSTALLINITY AND CRYSTAL SIZE

Several experiments were carried out to assess the effect of the thermal process on the synthesis. However the most remarkable parameter seems to be the heating rate, in such a way that lowering the heating rate promotes a substantial increase in crystallinity and in the average crystal size. In this respect, Figures S6.1-6.4 show a comparison of the SEM images and XRPD patterns of compounds $\{[M(Im)_2]\cdot(Py)_{0.5}\}_n$ [M(II): Co, Zn] prepared following thermal processes 1 and 3, respectively (further details in Tables S1.1 and S1.2). In the both cases the thermal process with the lower heating rate (3) leads to greater crystal size and greater crystallinity: the average crystal size of $\{[Co(Im)_2]\cdot(Py)_{0.5}\}_n$ range from 10 to 100 μm (a portion of smaller crystals is also present), while $\{[Zn(Im)_2]\cdot(Py)_{0.5}\}_n$ appears as somewhat smaller crystals (5 – 30 μm). However, an increase in the heating rate (thermal process *1*) during the synthesis stage, promoted a pronounced reduction of the crystal sizes (generally below 10 μm in both compounds) and crystallinity.

In the case of the sample prepared using the stoichiometric ratio Co:Im:4mPy 1:2.1:2.5, thermal process *3* leads to the formation of X-ray quality single crystals which allowed the structural determination of this compound that is reported in section S7.

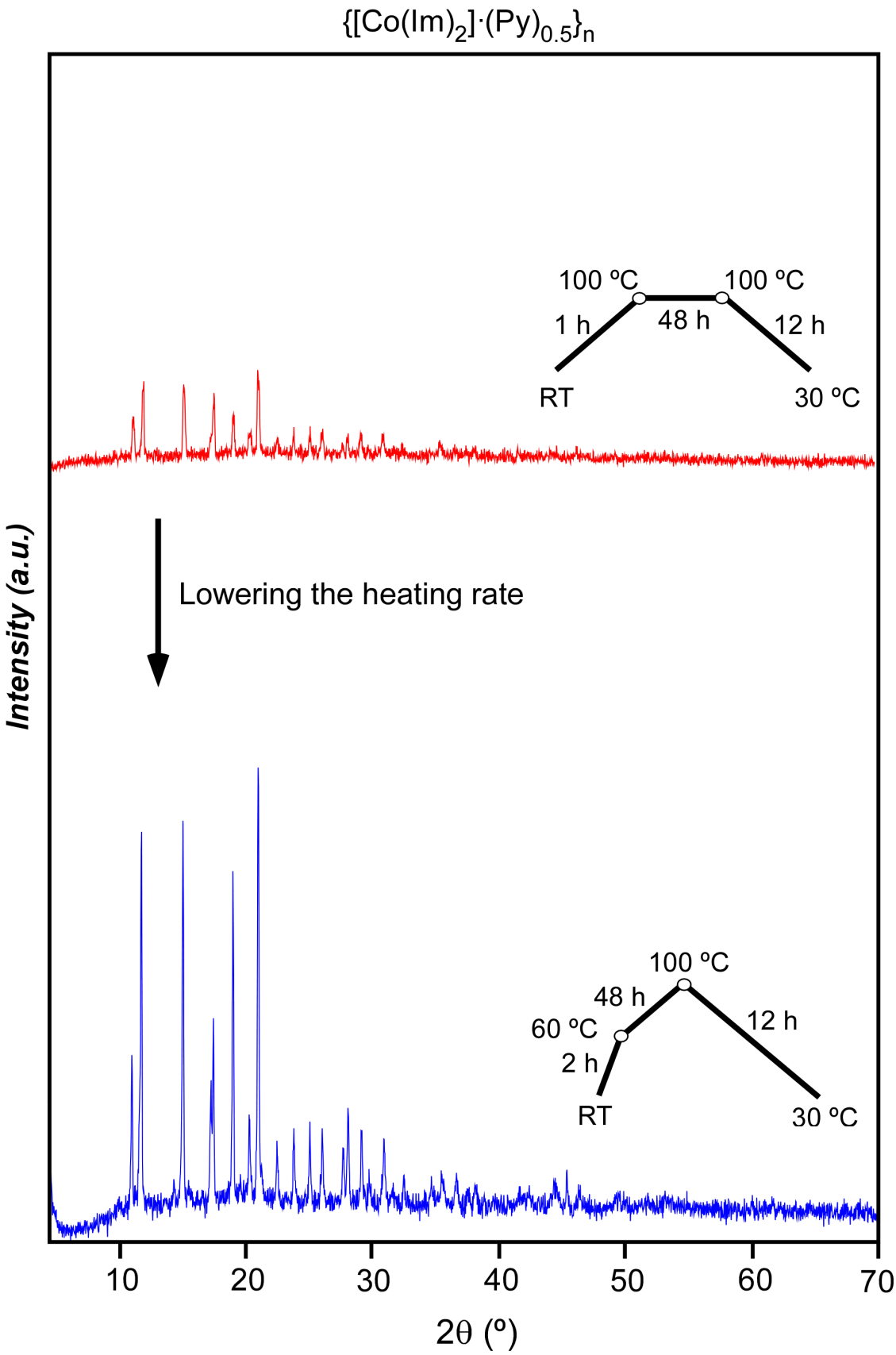

Figure S6.1. XRPD patterns of $\{[Co(Im)_2]\cdot(Py)_{0.5}\}_n$ prepared according to the thermal process *1* (a) and *3* (b). Non peaks of $Co(OH)_2$ where detected on the XRPD pattern.

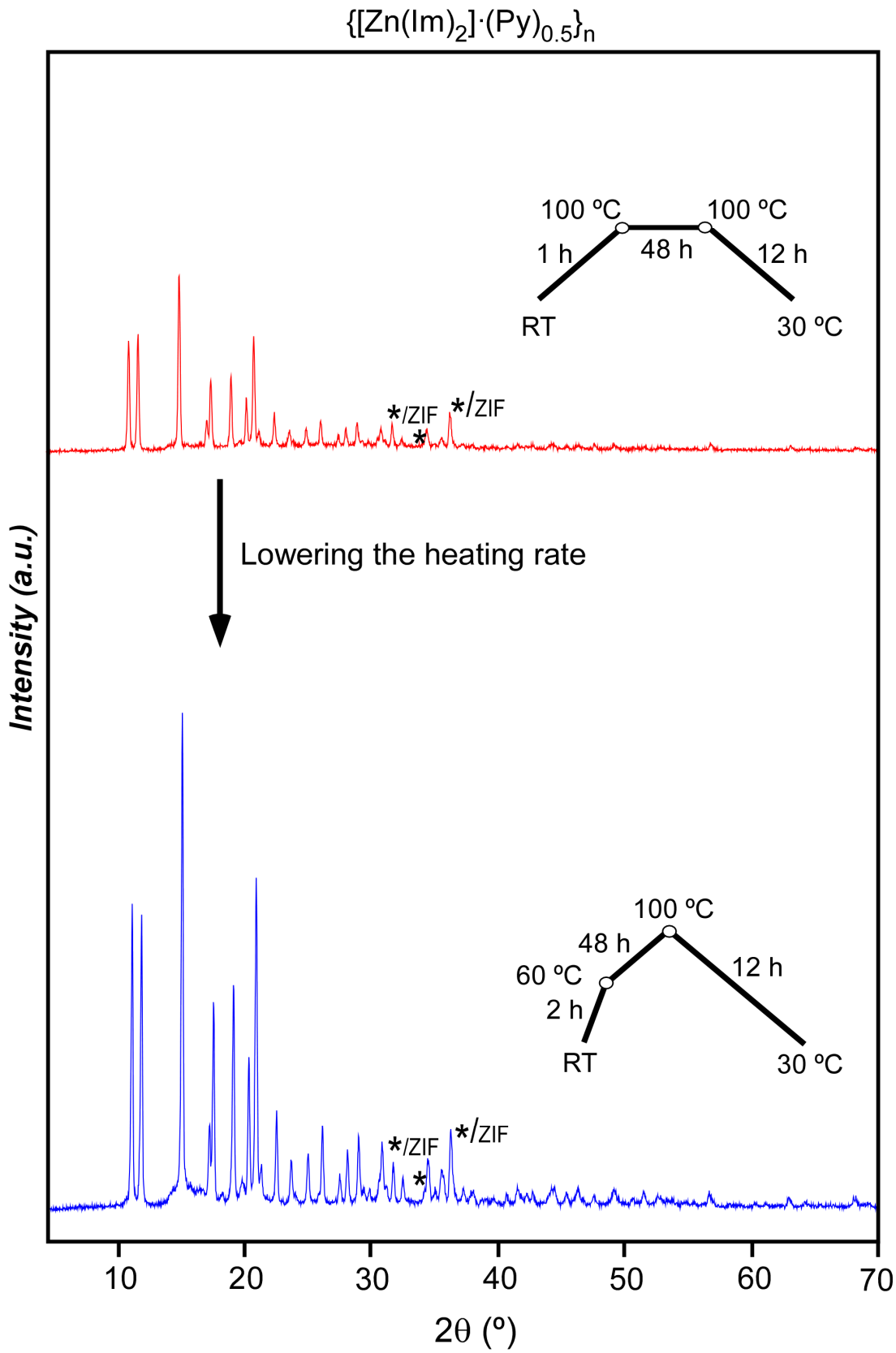

Figure S6.2. XRPD patterns of $\{[Zn(Im)_2]\cdot(Py)_{0.5}\}_n$ prepared according to the thermal process *1* (a) and *3* (b). "*" indicates the most intense peaks of ZnO, while "/ZIF" indicates overlaying with peaks corresponding to the zeolitic imidazalote framework.

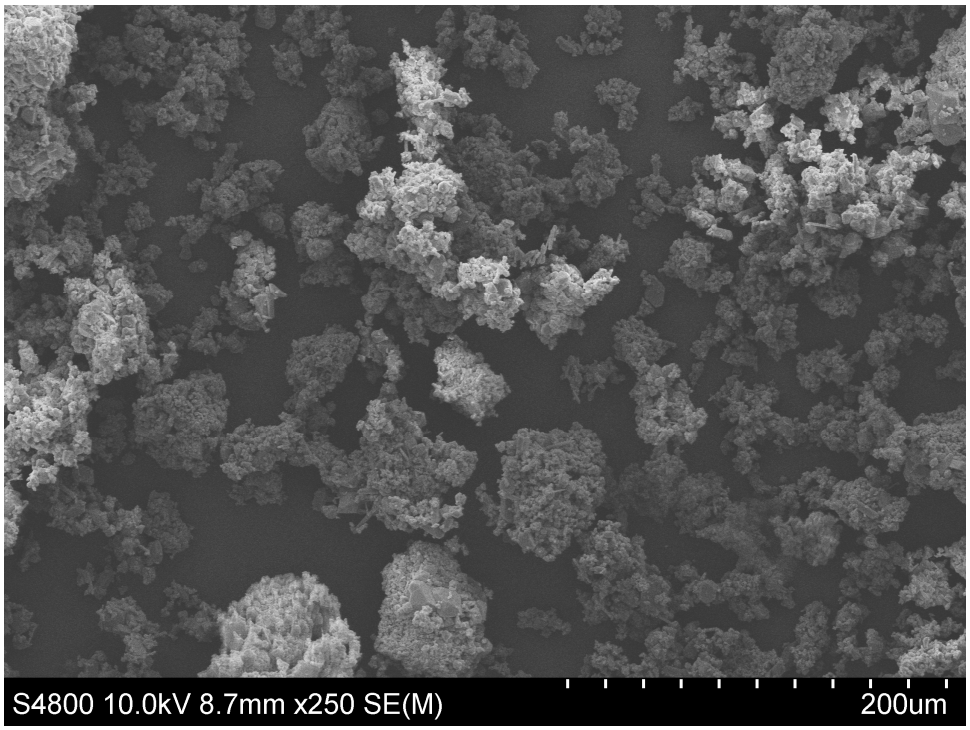

(a)

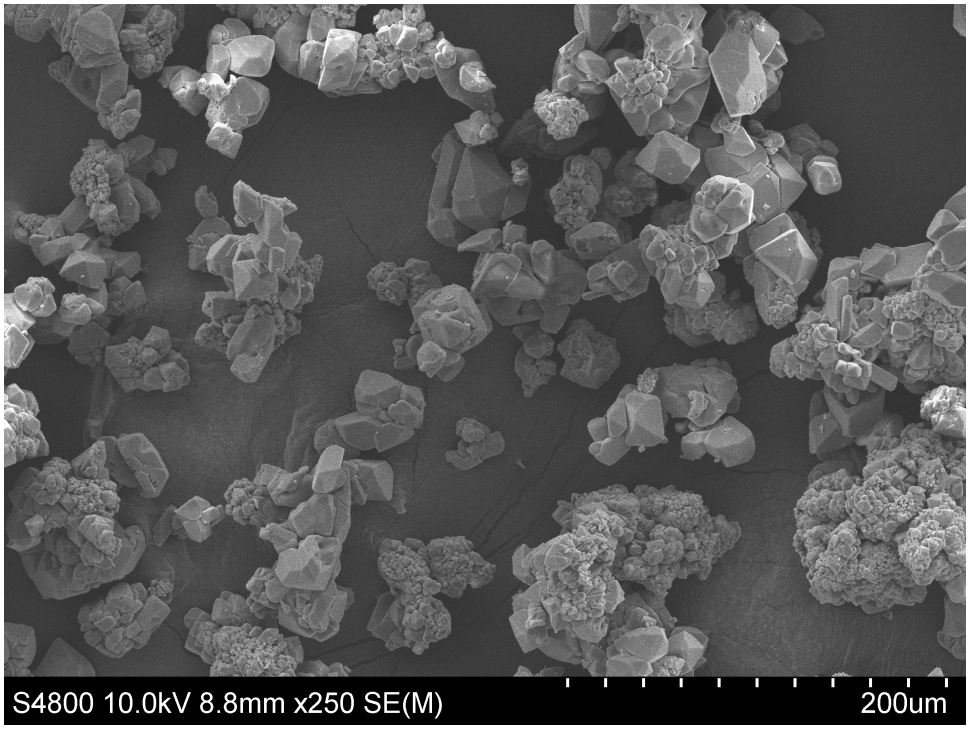

(b)

Figure S6.3. SEM images of $\{[Co(Im)_2]\cdot(Py)_{0.5}\}_n$ prepared according to the thermal process 1 (a) and 3 (b).

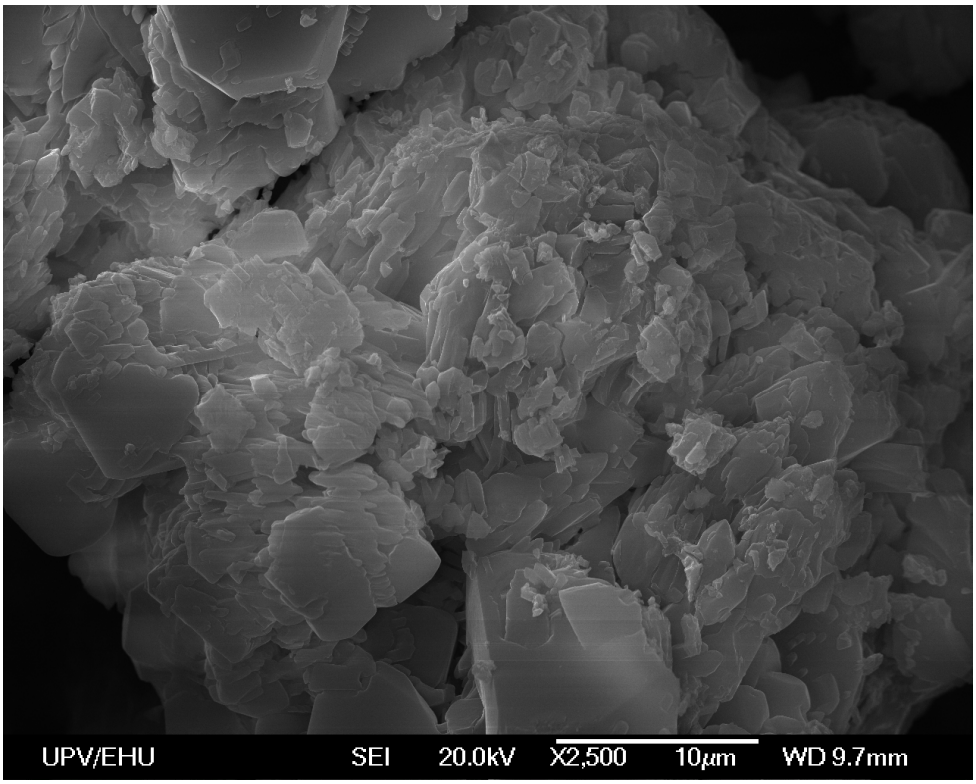

(a)

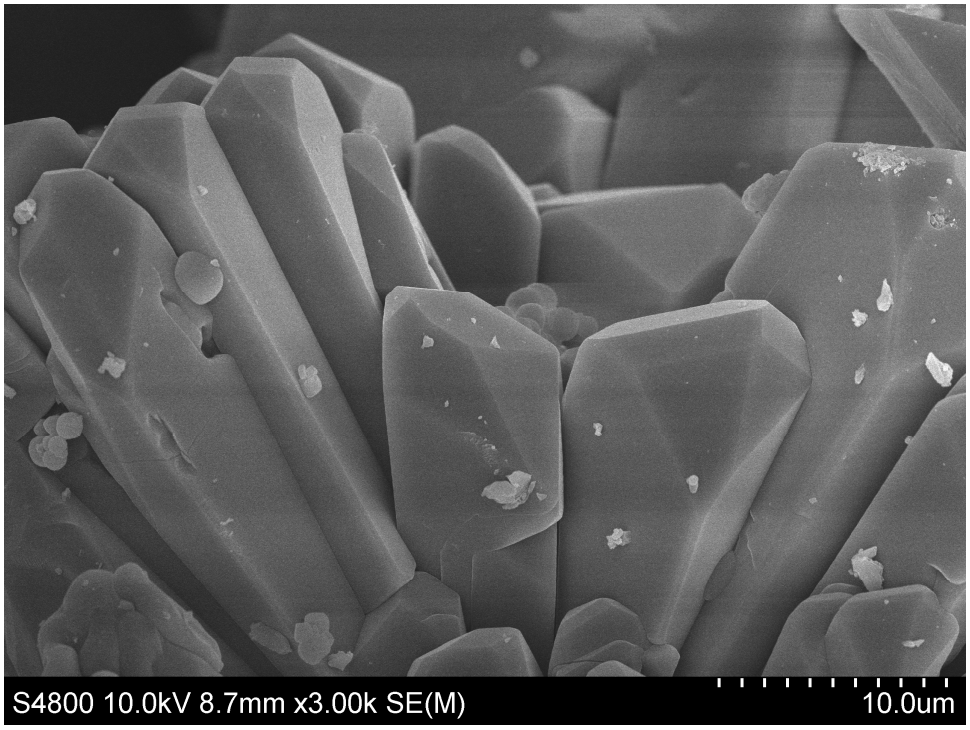

(b)

Figure S6.4. SEM images of $\{[Zn(Im)_2]\cdot(Py)_{0.5}\}_n$ prepared according to the thermal process *1* (a) and *3* (b).

S7. SINGLE CRYSTAL X-RAY DIFFRACTION DATA COLLECTION AND STRUCTURE DETERMINATION OF COMPOUND $\{[Co(Im)_2]\cdot(H_2O)_{2.5}\cdot(4mPy)_{0.2}\}_n$

X-ray Diffraction Data Collection and Structure Determination. Single crystal x-ray diffraction data of $\{[Co(Im)_2]\cdot(H_2O)_{2.5}\cdot(4mPy)_{0.2}\}_n$ were collected at 100(2) K on an Oxford Diffraction Xcalibur diffractometer with graphite-monochromated Mo-Kα radiation (λ = 0.71073 Å). The data reduction was done with the CrysAlis RED program.[3] The crystal structure was solved by direct methods using the SIR92 program[4] and refined by full-matrix least-squares on F^2 including all reflections (SHELXL97).[5] After completing the initial structure solution, the difference Fourier map showed the presence of substantial electron density at the voids of the structures that was impossible to model. Therefore, its contribution was subtracted from the reflection data by the SQUEEZE method[6] as implemented in PLATON.[7] The electron density subtracted by the SQUEEZE procedure is in agreement with the proposed content of the channels and it agrees to with the TG data. All the calculations for these structures were performed using the WINGX crystallographic software package.[8] Crystallographic data and structure refinement details are gathered in Table S7.1. In Figure S7.1 a fragment of metal-organic framework and a view of the crystal structure are provided.

Table S7.1. Crystallographic data and refinement details of $\{[Co(Im)_2]\cdot(H_2O)_{2.5}\cdot(4mPy)_{0.2}\}_n$.

Empirical formula	$C_{36}H_{53}Co_5N_{21}O_8$
Formula weight	1202.64
Crystal system	moniclinic
Space group	$P2_1/n$
a (Å)	24.3302(11)
b (Å)	9.5626(5)
c (Å)	24.6111(16)
β (°)	91.542(5)
V (Å^3)	5723.8(5)
Z	4
ρcalcd (g cm^{-3})	1.396
μ (mm^{-1})	11.624
Reflections collected	21401
Unique data/parameters	10225/496
R_{int}	0.1220
Goodness of fit (S)[a]	0.754
R_1[b]/wR_2[c] [I>2σ(I)]	0.0634/0.1361
R_1[b]/wR_2[c] [all data]	0.1221/0.1551

[a]$S = [\sum w(F_0^2 - F_c^2)^2 / (N_{obs} - N_{param})]^{1/2}$ [b]$R1 = \sum||F_0|-|F_c|| / \sum|F_0|$; [c]$wR2 = [\sum w(F_0^2 - F_c^2)^2 / \sum wF_0^2]^{1/2}$; $w = 1/[\sigma^2(F_0^2) + (aP)^2 + bP]$ where $P = (\max(F_0^2,0) + 2Fc^2)/3$ with a = 0.0534.

[3] *CrysAlis RED*, version 1.171.33.55; Oxford Diffraction: Wroclaw, Poland, **2010**.
[4] A. Altomare, M. Cascarano, C. Giacovazzo, A. Guagliardi, *J. Appl. Cryst.* **1993**, *26*, 343–350.
[5] G. M. Sheldrick, *SHELXL-97, Programs for X-ray Crystal Structure Refinement*; University of Göttingen, Germany, **1997**.
[6] P. Van der Sluis, A. L. Spek, *Acta Crystallogr.*, **1990**, *A46*, 194.
[7] A. L. Spek, *J. Appl. Cryst.*, **2003**, *36*, 7.
[8] L. J. Farrugia, *J. Appl. Cryst.* **1999**, *32*, 837.

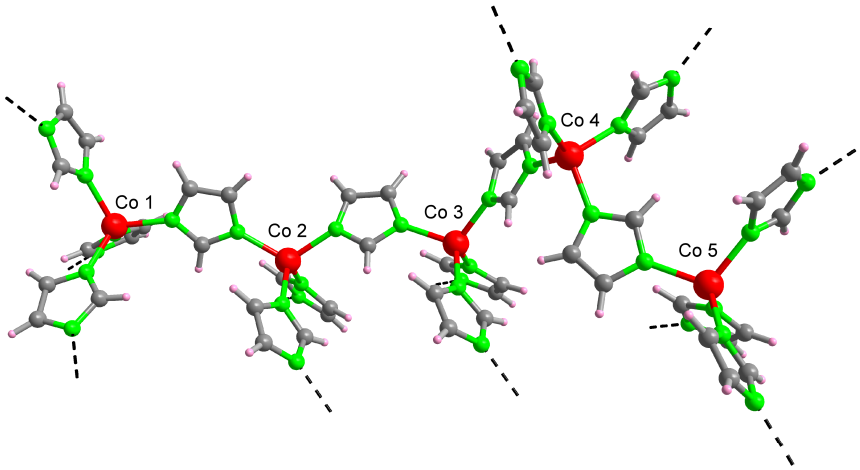

(a)

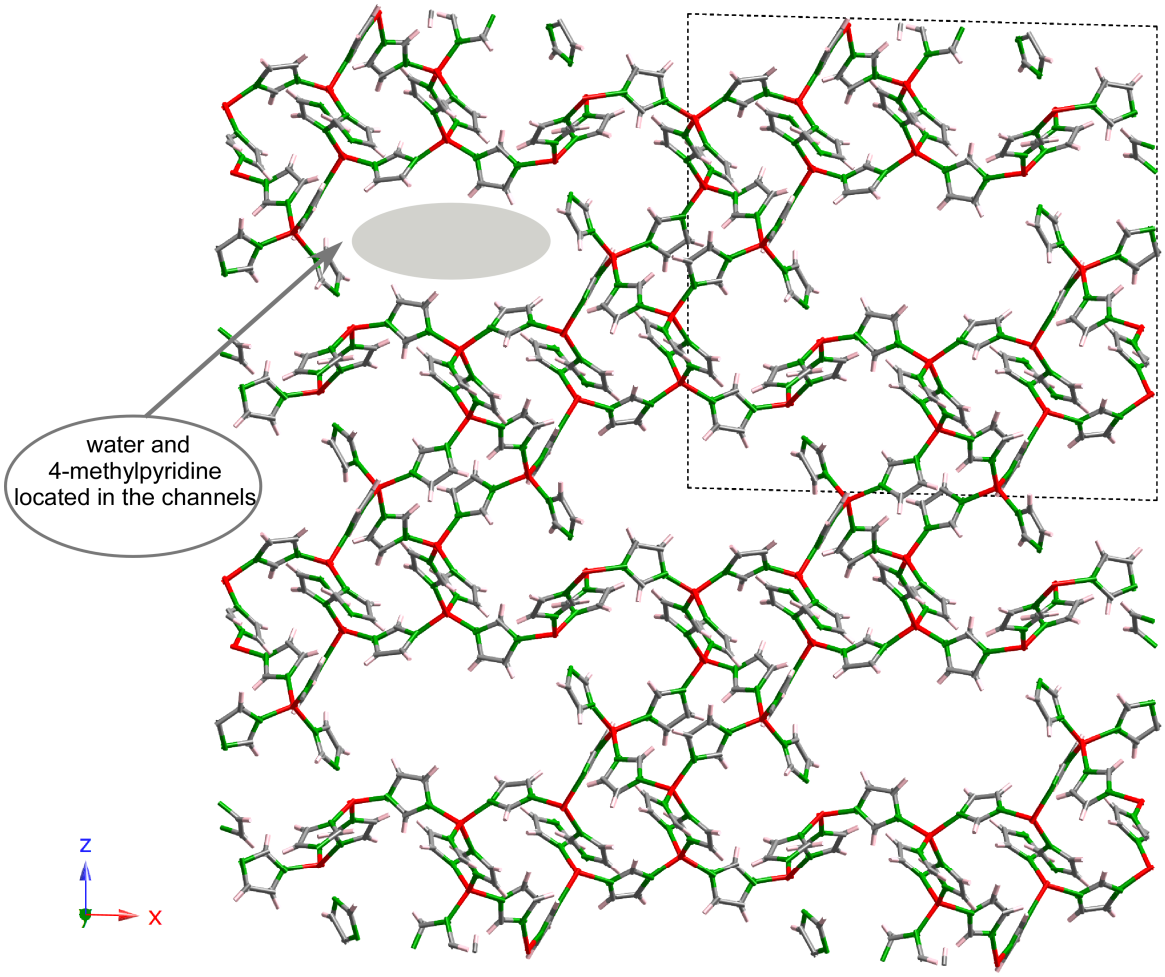

(b)

Figure S7.1. (a) A fragment showing the connectivity among the metal centers in the asymmetric unit of compound $\{[Co(Im)_2]\cdot(H_2O)_{2.5}\cdot(4mPy)_{0.2}\}_n$ and (b) a view of its crystal structure through [010] direction.

S8. N_2 ADSORPTION EXPERIMENTS

The permanent porosity of compounds $[M(mIm)_2]_n$ (M(II): Co, Zn; prepared from ZnO, $Co(OH)_2$) was studied by means of the measurements of N_2 adsorption isotherms at 77 K (Figure S8.1) using a *Micromeritics* ASAP 2010 analyser. Both samples were dried under vacuum at 150ºC during eight hours to eliminate solvent guest molecules prior to measurements. The crystallinity of the outgassed samples was retained as confirmed by XRPD measurements. The adsorption curves show two steps that are attributed to a structural change upon the N_2 adsorption at 77K. This behaviour has been previously reported for $[Zn(mIm)_2]_n$.[9] The adsorbed amount at $P/P_0 = 0.3$ is 495.9 cm^3/g (22.2 mmol/g) for $[Zn(mIm)_2]_n$ and is 521.9 cm^3/g (23.3 mmol/g) for $[Co(mIm)_2]_n$. The surface area values obtained by the fittings of the adsorption data BET equation were 1961 and 2070 m^2/g, respectively.

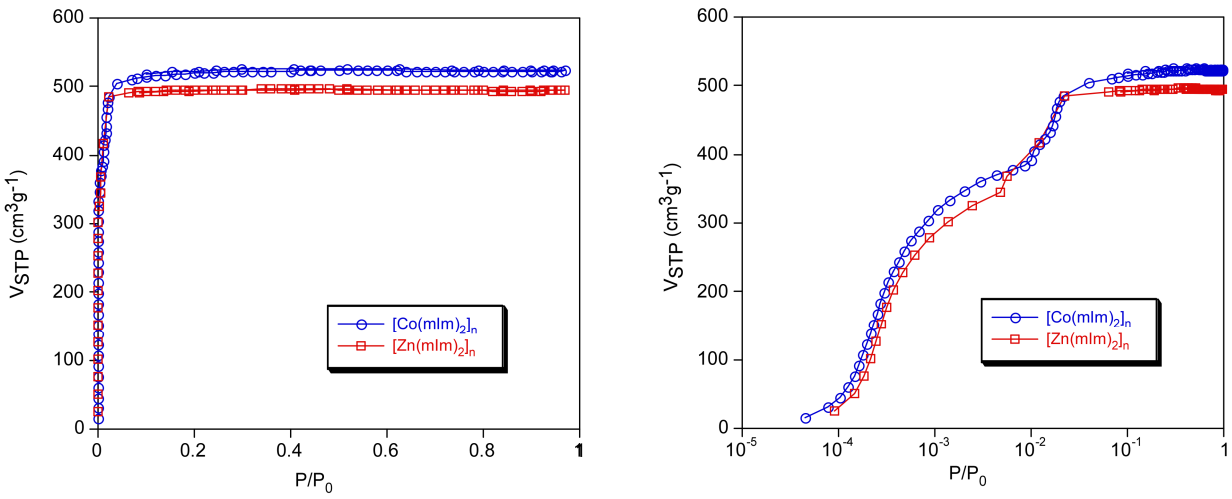

(a) (b)

Figure S8.1. Nitrogen adsorption isotherms at 77 K for outgassed compounds: (a) linear scale and (b) logarithmic scale.

[9] (a) D. Fairen-Jiménez, S. A. Moggach, M. T. Wharmby, P. A. Wright, S. Parsons, T. Duren, *J. Am. Chem. Soc.*, **2011**, *133*, 8900. (b) C. O. Ania, E. García-Pérez, M. Haro, J. J. Gutiérrez-Sevillano, T. Valdés-Solís, J. B. Parra‡, S. Calero, *J . Phys. Chem. Lett.*, **2012**, *3*, 1159.